



ELSEVIER

Physica A 273 (1999) 46–69

PHYSICA A

www.elsevier.com/locate/physa

# Scaling in nature: from DNA through heartbeats to weather

S. Havlin<sup>a,b,\*</sup>, S.V. Buldyrev<sup>a</sup>, A. Bunde<sup>c</sup>, A.L. Goldberger<sup>d</sup>,  
P.Ch. Ivanov<sup>a,d</sup>, C.-K. Peng<sup>a,d</sup>, H.E. Stanley<sup>a</sup>

<sup>a</sup>Center for Polymer Studies and Department of Physics, Boston University, Boston, MA 02215, USA

<sup>b</sup>Gonda-Goldschmied Center and Department of Physics, Bar-Ilan University, Ramat-Gan 52900, Israel

<sup>c</sup>Institut für Theoretische Physik III, Justus-Liebig-Universität Biessen, Heinrich-Buff-Ring 16,  
35392 Giessen, Germany

<sup>d</sup>Cardiovascular Division, Harvard Medical School, Beth Israel Hospital, Boston, MA 02215, USA

Received 9 August 1999

---

## Abstract

The purpose of this report is to describe some recent progress in applying scaling concepts to various systems in nature. We review several systems characterized by scaling laws such as DNA sequences, heartbeat rates and weather variations. We discuss the finding that the exponent  $\alpha$  quantifying the scaling in DNA is smaller for coding than for noncoding sequences. We also discuss the application of fractal scaling analysis to the dynamics of heartbeat regulation, and report the recent finding that the scaling exponent  $\alpha$  is smaller during sleep periods compared to wake periods. We also discuss the recent findings that suggest a universal scaling exponent characterizing the weather fluctuations. © 1999 Elsevier Science B.V. All rights reserved.

*PACS:* 87.10.+e; 87.80.+s; 87.90.+y; 05.40.+j

*Keywords:* DNA; Heartbeat; Weather; Time series; Scaling; Fractals

---

## 0. Introduction

In the last decade it was realized that many systems in nature have no characteristic length or time scale, i.e., they have fractal — or, more generally, scaling — properties [1–15]. However, the fractal properties in different systems, have quite different nature, origin, and appearance. In some cases, it is the geometrical shape of an object itself

---

\* Correspondence address. Center for Polymer Studies and Department of Physics, Boston University, Boston, MA 02215, USA. Fax: +972-3-535-7678.

*E-mail address:* havlin@ophir.ph.biu.ac.il (S. Havlin)

that exhibits obvious fractal features, while in other cases the fractal properties are more “hidden” and can only be perceived if data are studied as a function of time or mapped onto a graph in some special way. After an appropriate mapping, such a graph may resemble a mountain landscape, with jagged ridges of all length scales from very small bumps to enormous peaks. Mathematically, these landscapes can be quantified in terms of fractal and scaling concepts such as self-affinity. The range of systems that apparently display power-law and hence scale-invariant correlations have increased dramatically in recent years, ranging from base pair correlations in deoxyribonucleic acid (DNA) [16], lung inflation [17,18] and interbeat intervals of the human heart [19–23] to complex systems involving large numbers of interacting subunits that display “free will”, such as city growth [24], weather fluctuations [25] and even economics [26–28]. The main purpose of this paper is devoted to the study of such hidden fractal properties that have been recently discovered in DNA sequences, heartbeat activity and weather fluctuations. The common feature of these three topics is the long-range power-law correlations which have been found in these systems.

## 1. DNA

The role of genomic DNA sequence in coding for protein structure is well known [29,30]. The human genome contains information for approximately 100,000 different proteins, which define all inheritable features of an individual. The genomic sequence is likely the most sophisticated information database created by nature through the dynamic process of evolution. Equally remarkable is the precise transformation of information (duplication, decoding, etc.) that occurs in a relatively short time interval.

In order to study the scale-invariant long-range correlations of a DNA sequence, we first introduced a graphical representation of DNA sequences, which we term a *fractal landscape* or *DNA walk* [16]. For the conventional one-dimensional random walk model [31,32], a walker moves either “up” [ $u(i) = +1$ ] or “down” [ $u(i) = -1$ ] one unit length for each step  $i$  of the walk. For the case of an uncorrelated walk, the direction of each step is independent of the previous steps. For the case of a correlated random walk, the direction of each step depends on the history (“memory”) of the walker [33–36].

One definition of the DNA walk is that the walker steps “up” if a pyrimidine (C or T) occurs at position  $i$  along the DNA chain, while the walker steps “down” if a purine (A or G) occurs at position  $i$ . The question we asked was whether such a walk displays only short-range correlations (as in an  $n$ -step Markov chain) or long-range correlations (as in critical phenomena and other scale-free “fractal” phenomena). A similar kind of DNA walk was suggested by Azbel [37].

There have also been attempts to map DNA sequence onto multi-dimensional DNA walks [38,39]. However, recent work [40,41] indicates that the original purine-pyrimidine rule provides the most robust results, probably due to the purine-pyrimidine chemical complementarity.

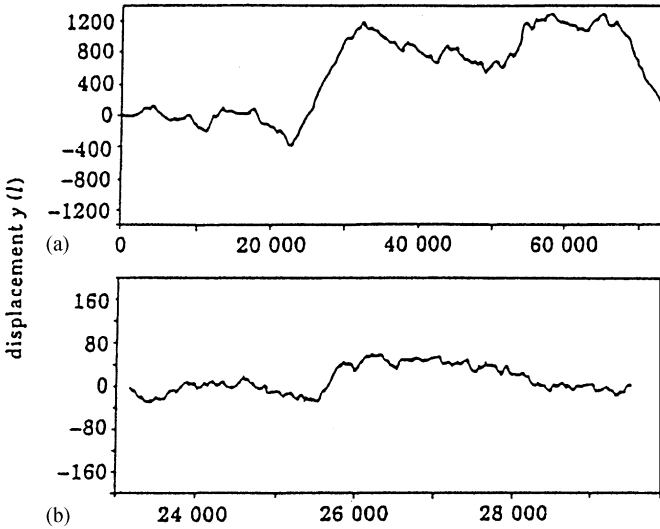


Fig. 1. DNA walk displacement  $y(\ell)$  (excess of purines over pyrimidines) vs. nucleotide distance  $\ell$  for (a) HUMHBB (human beta globin chromosomal region of the total length  $L = 73\,239$ ); (b) the LINE1c region of HUMHBB starting from 23 137 to 29 515. This sub-segment is a Markovian random walk. Note that in all cases the overall bias was subtracted from the graph such that the beginning and ending points have the same vertical displacement ( $y = 0$ ). This was done to make the graphs clearer and does not affect the quantitative analysis of the data. Courtesy of S.V. Buldyrev et al. [56,108].

An important statistical quantity characterizing any walk [31,32] is the root mean-square fluctuation  $F(\ell)$  about the average of the displacement of a quantity  $\Delta y(\ell)$  defined by  $\Delta y(\ell) \equiv y(\ell_0 + \ell) - y(\ell_0)$ , where

$$y(\ell) \equiv \sum_{i=1}^{\ell} u(i). \quad (1)$$

If there is no characteristic length (i.e., if the correlation were “infinite-range”), then fluctuations will also be described by a power law

$$F(\ell) \sim \ell^{\alpha} \quad (2)$$

with  $\alpha \neq \frac{1}{2}$ . The value  $\alpha = \frac{1}{2}$  correspond to short-range correlations.

Figure 1 shows a typical example of a gene that contains a significant fraction of base pairs that do *not* code for amino acids. It is immediately apparent that the DNA walk has an extremely jagged contour which corresponds to long-range correlations.

The fact that data for intron-containing and intergenic (i.e., noncoding) sequences are linear on double logarithmic plot confirms that  $F(\ell) \sim \ell^{\alpha}$ . A least-squares fit produces a straight line with slope  $\alpha$  substantially larger than the prediction for an uncorrelated walk,  $\alpha = \frac{1}{2}$ , thus providing direct experimental evidence for the presence of long-range correlations.

On the other hand, the dependence of  $F(\ell)$  for coding sequences is not linear on the log–log plot: its slope undergoes a crossover from 0.5 for small  $\ell$  to 1 for large  $\ell$ . However, if a single patch is analyzed separately, the log–log plot of  $F(\ell)$  is again

a straight line with the slope close to 0.5. This suggests that within a large patch the coding sequence is almost uncorrelated. The function  $F(\ell)$  was also studied for DNA sequences by Azbel [42], who identified qualitatively the presence of long-range correlations.

## 2. Detrended fluctuation analysis (DFA) applied to DNA

The initial report [16,38] on long-range (scale-invariant) correlations only in non-coding DNA sequences has generated contradicting responses. Some [43–45] support our initial finding, while some [46–54] disagree. However, the conclusions of Refs. [46–54] are inconsistent *with one another* in which Nee [46] and Karlin and Brendel [54] doubt the existence of long-range correlations (even in noncoding sequences) while Voss [47], Prabhu and Claverie [49] and Chatzidimitriou Dreismann et al. [50–53] conclude that even coding regions display long-range correlations ( $\alpha > \frac{1}{2}$ ). Prabhu and Claverie [49] claim that their analysis of the putative *coding* regions of the yeast chromosome III produces a *wide range of exponent values*, some larger than 0.5. The source of these contradicting claims may arise from the fact that, in addition to normal statistical fluctuations expected for analysis of rather short sequences, coding regions typically consist of only a few lengthy regions of alternating strand bias — and so we have nonstationarity. Hence conventional scaling analyses cannot be applied reliably to the entire sequence but only to sub-sequences.

Peng et al. [55] have developed a method specifically adapted to handle problems associated with nonstationary sequences which they term *detrended fluctuation analysis* (DFA).

The idea of the DFA method is to compute the dependence of the standard error of a linear interpolation of a DNA walk  $F_d(\ell)$  on the size of the interpolation segment  $\ell$ . The method takes into account differences in local nucleotide content and may be applied to the entire sequence which has lengthy patches. In contrast with the original  $F(\ell)$  function, which has spurious crossovers even for  $\ell$  much smaller than a typical patch size, the detrended function  $F_d(\ell)$  shows linear behavior on the log–log plot for all length scales up to the characteristic patch size, which is of the order of a thousand nucleotides in the coding sequences. For  $\ell$  close to the characteristic patch size the log–log plot of  $F_d(\ell)$  has an abrupt change in its slope.

The DFA method clearly supports the difference between coding and noncoding sequences, showing that the coding sequences are less correlated than noncoding sequences for the length scales less than 1000, which is close to characteristic patch size in the coding regions. Buldyrev et al. [56] analyzed using DFA all 33 301 coding and all 29 453 noncoding eukaryotic sequences — each of length larger than 512 base pairs (bp) — in the 1995 release of the GenBank to determine whether there is any statistically significant distinction in their long-range correlation properties.

Buldyrev et al. [56] find that standard fast Fourier transform (FFT) analysis indicates that *coding* sequences have practically no correlations in the range from 10 to 100 bp

(spectral exponent  $\beta \pm 2SD = 0.00 \pm 0.04$ ). Here  $\beta$  is defined through the relation  $S(f) \sim 1/f^\beta$ , where  $S(f)$  is the Fourier transform of the correlation function, and  $\beta$  is related to the long-range correlation exponent  $\alpha$  by  $\beta = 2\alpha - 1$  so that  $\alpha = \frac{1}{2}$  corresponds to  $\beta = 0$  (white noise). In contrast, for *noncoding* sequences, the average value of the spectral exponent  $\beta$  is positive ( $0.16 \pm 0.05$ ), which unambiguously shows the presence of long-range correlations. The near-perfect agreement between the two independent analysis methods, FFT and DFA, increases the confidence in the reliability of the conclusion of long-range correlation properties of coding and noncoding sequences.

From a practical viewpoint, the statistically significant difference in long-range power-law correlations between coding and noncoding DNA regions that we observe supports the development of gene finding algorithms based on these distinct scaling properties. A reported algorithm of this kind [40,41] is especially useful in the analysis of DNA sequences with relatively long coding regions, such as those in yeast chromosome III.

Arneodo et al. [57,58] studied long-range correlation in DNA sequences using wavelet analysis. The wavelet transform can be made blind to “patchiness” of genomic sequences. They found the existence of long-range correlations in noncoding regimes, and no long-range correlations in coding regimes in excellent agreement with Buldyrev et al. [56].

Very recently, Thermes et al. [59] by means of wavelet analysis found universal multi-scale properties of genomic DNA. They relate these scaling properties to the structural organization of the DNA molecule. Such relation was also suggested by Grosberg et al. [45].

### 3. Scaling analysis of heartbeat intervals

The idea of long-range correlations has been applied to the analysis of the beat-to-beat intervals in the normal and diseased heart [22]. The healthy heartbeat is generally thought to be regulated according to the classical principle of homeostasis whereby physiologic systems operate to reduce variability and achieve an equilibrium-like state [60]. We find, however, that under normal conditions, beat-to-beat fluctuations in heart rate display the kind of long-range correlations typically exhibited by physical dynamical systems far from equilibrium, such as those near a critical point. We review recently reported evidence for such power-law correlations that extend over thousands of heart-beats in healthy subjects. In contrast, heart rate time series from patients with severe congestive heart failure show a breakdown of this long-range correlation behavior, with the emergence of a characteristic short-range time scale. Such alterations in correlation behavior may be important in modeling the transition from health to disease in a wide variety of pathologic conditions.

Normal activity of the heart is usually described as “regular sinus rhythm” [61–64]. However, as shown in Fig. 2, cardiac interbeat intervals fluctuate in an irregular manner in healthy subjects — even at rest or during sleep [65]. The complex behavior of the heartbeat manifests itself through the nonstationarity and nonlinearity of interbeat

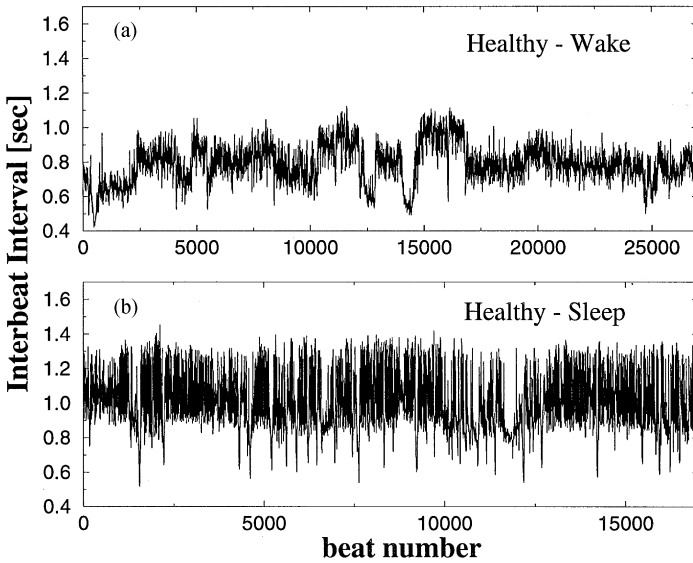


Fig. 2. Consecutive heartbeat intervals vs. beat number are plotted for 6 h recorded for the same healthy subject during: (a) wake period: 12 p.m. to 6 p.m. and (b) sleep period: 12 a.m. to 6 a.m. (Note that there are fewer interbeat intervals during sleep due to the larger average of the interbeat intervals, i.e. slower heart rate.) Courtesy of P.Ch. Ivanov et al. [83].

interval sequences [66–68]. In recent years, the intriguing statistical properties of interbeat interval sequences have attracted the attention of researchers from many fields [69–74].

Initially, analysis of heartbeat fluctuations focused on short time oscillations associated with breathing, blood pressure and neuroautonomic control [75]. Studies of longer heartbeat records, however, revealed  $1/f$ -like behavior [19,76]. Recent analysis of very long time series (up to 24 h:  $n \approx 10^5$  beats) show that under healthy conditions, interbeat interval increments exhibit power-law anticorrelations [22] and follow a universal scaling form in their distributions [77]. These scaling features change with disease and advanced age [78–80]. The emergence of scale-invariant properties in the seemingly “noisy” heartbeat fluctuations is believed to be a result of highly complex, nonlinear mechanisms of physiologic control [81].

It is known that circadian rhythms are associated with periodic changes in key physiological processes [64,65,82]. Here, we review a recent study [83] asking if there are characteristic differences in the scaling behavior between sleep and wake cardiac dynamics. Typically, the differences in the cardiac dynamics during sleep and wake phases are reflected in the average (higher in sleep) and standard deviation (lower in sleep) of the interbeat intervals [82]. Such differences can be easily observed in plots of the interbeat intervals recorded from subjects during sleep and wake periods (Fig. 2). The hypothesis is that sleep and wake changes in cardiac control may occur on all time scales and thus could lead to systematic changes in the scaling properties of

the heartbeat dynamics. Elucidating the nature of these sleep–wake rhythms could lead to a better understanding of the neuroautonomic mechanisms of cardiac regulation.

Ivanov et al. [83] analyzed 30 databases — each with 24 h of interbeat intervals — from 18 healthy subjects and 12 patients with congestive heart failure [98]. The nocturnal and diurnal fractions of the dataset of each subject correspond to the 6 h ( $n \approx 22,000$  beats) from midnight to 6 a.m. and from noon to 6 p.m.

The detrended fluctuation analysis (DFA) method [55] has been applied to quantify long-range correlations embedded in the nonstationary heartbeat time series. This method avoids spurious detection of correlations that are artifacts of nonstationarity. Briefly, we first integrate the interbeat interval time series and then divide it into boxes of equal length,  $n$ . In each box, we fit the data with a least-squares line which represents the local trend in that box. Next we detrend the integrated time series by subtracting the local trend in each box. We calculate the root-mean-square fluctuation  $F(n)$  of this integrated and detrended time series for different time scales (box sizes)  $n$ . A power-law relation between the average fluctuation  $F(n)$  and the number of beats  $n$  in a box indicates the presence of scaling; the correlations in the heart-beat fluctuations can be characterized by the scaling exponent  $\alpha$ , defined as  $F(n) \sim n^\alpha$ , see Eq. (2).

Ref. [83] finds that at scales above  $\approx 1$  min ( $n > 60$ ) the data during wake hours display long-range correlations over two decades with average exponents  $\alpha_W \approx 1.05$  for the healthy group and  $\alpha_W \approx 1.2$  for the heart failure patients. For the sleep data, we systematically find a crossover at scale  $n \approx 60$  beats, followed by a scaling regime extending over two decades characterized by a smaller exponent:  $\alpha_S \approx 0.85$  for the healthy group and  $\alpha_S \approx 0.95$  for the heart failure group (Fig. 3). Although the values of the sleep and wake exponents vary from subject to subject, we find [83] that for all individuals studied, the heartbeat dynamics during sleep are characterized by a smaller exponent (Table 1).

As a control, an identical analysis is performed on two surrogate data sets obtained by reshuffling and integrating the increments in the interbeat intervals of the sleep and

Table 1

Comparison of the statistics for the scaling exponents from the three groups in our database. Here  $N$  is the number of datasets in each group,  $\alpha$  is the corresponding group average value and  $\sigma$  is the standard deviation of the exponent values for each group. The differences between the average sleep and wake-phase exponents for all three groups are statistically significant ( $p < 10^{-5}$  by the Student's  $t$ -test). Courtesy of P.Ch. Ivanov et al. [83].

Group	$N$	$\alpha$	$\sigma$
Healthy wake	18	1.05	0.07
Healthy sleep	18	0.85	0.10
Cosmonaut wake	17	1.04	0.12
Cosmonaut sleep	17	0.82	0.07
Heart failure wake	12	1.20	0.09
Heart failure sleep	12	0.95	0.15

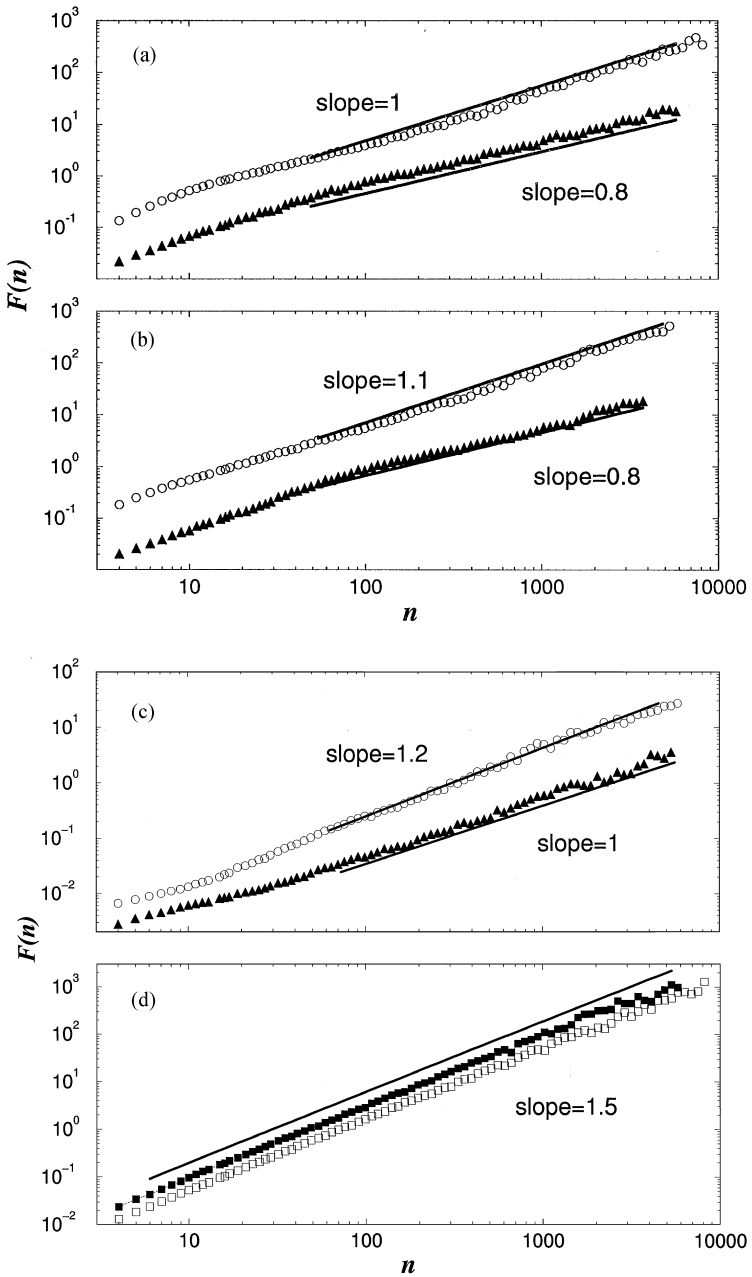


Fig. 3. Plots of  $\log F(n)$  vs.  $\log n$  for 6 h wake (open circles) and sleep records (filled triangles) of (a) one typical healthy subject; (b) one cosmonaut (during orbital flight); and (c) one patient with congestive heart failure. Note the systematic lower exponent for the sleep phase (filled triangles), indicating stronger anticorrelations. (d) As a control, we reshuffle and integrate the interbeat increments from the wake and sleep data of the healthy subject presented in (a). We find a Brownian noise scaling over all time scales for both wake and sleep phases with an exponent  $\alpha = 1.5$ , as one expects for random walk-like fluctuations. Courtesy of P.Ch. Ivanov et al. [83].

wake records from the same healthy subject presented in Fig. 3a. Both surrogate sets display uncorrelated random walk fluctuations with a scaling exponent of 1.5 (Brownian noise) (Fig. 3d). A scaling exponent larger than 1.5 would indicate persistent correlated behavior, while exponents with values smaller than 1.5 characterize anticorrelations (a perfectly anticorrelated signal would have an exponent close to zero). Our results therefore suggest that the interbeat fluctuations during sleep and wake phases are long-range anticorrelated but with a significantly greater degree of anticorrelation (smaller exponent) during sleep.

An important question is whether the observed scaling differences between sleep and wake cardiac dynamics arise trivially from changes in environmental conditions (different daily activities are reflected in the strong nonstationarity of heartbeat time series). Environmental “noise”, however, can be treated as a “trend” and distinguished from the more subtle fluctuations that may reveal intrinsic correlation properties of the dynamics. Alternatively, the interbeat fluctuations may arise from nonlinear dynamical control of the neuroautonomic system rather than being an epiphenomenon of environmental stimuli, in which case only the fluctuations arising from the intrinsic dynamics of the neuroautonomic system should show long-range scaling behavior.

The analysis in Ref. [83] suggests that the observed sleep–wake scaling differences are due to intrinsic changes in the cardiac control mechanisms for the following reasons: (i) The DFA method removes the “noise” due to activity by detrending the nonstationarities in the interbeat interval signal and analyzing the fluctuations along the trends. (ii) Responses to external stimuli should give rise to a different type of fluctuations having characteristic time scales, i.e., frequencies related to the stimuli. However, fluctuations in both diurnal and nocturnal cardiac dynamics exhibit scale-free behavior. (iii) The weaker anticorrelated behavior observed for all wake-phase records cannot be simply explained as a superposition of stronger anticorrelated sleep dynamics and random noise of day activity. Such noise would dominate at large scales and should lead to a crossover with an exponent of 1.5. However, such crossover behavior is not observed in any of the wake-phase datasets (Fig. 3). Rather, the wake dynamics are typically characterized by a stable scaling regime up to  $n = 5000$  beats.

The robustness of the above results was tested by analyzing 17 datasets from six cosmonauts during long-term orbital flight on the Mir space station [84]. Each dataset contains continuous periods of 6 h data under both sleep and wake conditions. We find that for all cosmonauts the heartbeat fluctuations exhibit anticorrelated behavior with average scaling exponents consistent with those found for the healthy terrestrial group:  $\alpha_W \approx 1.04$  for the wake phase and  $\alpha_S \approx 0.82$  for the sleep phase (Table 1). The sleep–wake scaling difference is observed not only for the group averaged exponents but for each individual cosmonaut dataset (Fig. 3b). Moreover, the scaling differences are persistent in time, since records of the same cosmonaut taken on different days (ranging from the 3rd to the 158th day in orbit), exhibit a higher degree of anticorrelation during sleep.

We find that even under the extreme conditions of zero gravity and high-stress activity, the sleep and wake scaling exponents for the cosmonauts are statistically

consistent ( $p = 0.7$  by Student's  $t$ -test) with those of the terrestrial healthy group [2]. Thus the larger values for the wake phase scaling exponents cannot be a trivial artifact of activity. Furthermore, the larger value of the average wake exponent for the heart failure group compared to the other two groups (Table 1) cannot be attributed to external stimuli either, since patients with severe cardiac disease are strongly restricted in their physical activity. Instead, our results suggest that the observed scaling characteristics in the heartbeat fluctuations during sleep and wake phases are related to intrinsic mechanisms of neuroautonomic control. The observed sleep-wake changes in the scaling characteristics may indicate different regimes of intrinsic neuroautonomic regulation of the cardiac dynamics, which may “switch” on and off associated with circadian rhythms.

Surprisingly, we note that for large time scales ( $n > 60$ ) the average sleep-wake scaling difference is comparable to the scaling difference between health and disease; cf. Table 1. At small time scales ( $n < 60$ ), we do not observe systematic sleep-wake differences. The scaling exponents obtained from 24 h records of healthy and heart failure subjects in the asymptotic region of large time scales are in agreement with the results for the healthy and heart failure groups during the wake phase only. Since the weaker anticorrelations associated with the wake phase are characterized by a larger exponent while the stronger anticorrelated behavior during sleep has a smaller exponent, at large scales the superposition of the two phases (in 24 h records) will exhibit behavior dominated by the larger exponent of the wake phase.

We also note that the scaling exponents for the heart failure group during sleep are close to the exponents observed for the healthy group (Table 1). Since heart failure occurs when the cardiac output is not adequate to meet the metabolic demands of the body, one would anticipate that the manifestations of heart failure would be most severe during physical stress when metabolic demands are greatest, and least severe when metabolic demands are minimal, i.e., during rest or sleep. The scaling results we obtain are consistent with these physiological considerations: the heart failure subjects should be closer to normal during minimal activity. Of related interest, recent studies indicate that sudden death in individuals with underlying heart disease is most likely to occur in the hours just after awakening [85,86]. Our findings raise the intriguing possibility that the transition between the sleep and wake phases is a period of potentially increased neuroautonomic instability because it requires a transition from strongly to weakly anticorrelated regulation of the heart.

The finding of stronger heartbeat anticorrelations during sleep is of interest from a physiological viewpoint, since it may motivate new modeling approaches and supports a reassessment of the sleep phase as a surprisingly active dynamical state. Perhaps the “restorative” functions of sleep may relate to an increased reflexive-type responsiveness of neuroautonomic control, not just at one characteristic frequency, but over a broad range of time scales.

Recent work by Ivanov et al. [87] indicates that key statistical characteristics of the healthy cardiac dynamics can be successfully reproduced by a stochastic nonlinear feedback mechanism. The present observation of sleep-wake scaling differences

poses a new challenge to such modeling approaches, which could require considering reciprocity in the activity of the sympathetic and parasympathetic branches of the autonomic nervous system during sleep and wake phases, as well as different correlation times of the sympathetic and parasympathetic impulses.

#### 4. Wavelet analysis of heartbeat intervals

Time series of beat-to-beat (RR) heart rate intervals (Fig. 4a) obtained from digitized electrocardiograms are known to be nonstationary and exhibit extremely complex behavior [88–90]. A typical feature of these signals is the presence of “patchy” patterns which change over time (Fig. 4b). Heterogeneous properties may be even more strongly expressed in certain cases of abnormal heart activity. Traditional approaches — such as the power spectrum and correlation analysis [91,92] — are not suited for such nonstationary (patchy) sequences, and do not carry information stored in the Fourier phases (crucial for determining nonlinear characteristics).

To address these problems, we present an alternative method — “*cumulative variation magnitude analysis*” [77] — to study the subtle structure of physiological time series. This method comprises sequential application of a set of algorithms based on wavelet and Hilbert transform analysis. First, we apply the wavelet transform (Fig. 4c), because it does not require stationarity and preserves the Fourier phase information. The wavelet transform [93–95] of a time series  $s(t)$  is defined as

$$T_{\psi}(t_0, a) \equiv a^{-1} \int_{-\infty}^{+\infty} s(t) \psi \left( \frac{t - t_0}{a} \right) dt, \quad (3)$$

where the analyzing wavelet  $\psi$  has a width of the order of the scale  $a$  and is centered at  $t_0$ . For high frequencies (small  $a$ ), the  $\psi$  functions have good localization (being effectively nonzero only on small sub-intervals), so short-time regimes or high-frequency components can be detected by the wavelet analysis. The wavelet transform is sometimes called a “mathematical microscope” because it allows one to study properties of the signal on any chosen scale  $a$ . However, a wavelet with too large a value of scale  $a$  (low frequency) will filter out almost the entire frequency content of the time series, thus losing information about the intrinsic dynamics of the system. We focus our “microscope” on scale  $a = 8$  beats which smoothes locally very high-frequency variations and best probes patterns of specific duration ( $\approx \frac{1}{2} - 1$  min) (Fig. 4). The wavelet transform is attractive because it can eliminate local polynomial behavior in the nonstationary signal by an appropriate choice of the analyzing wavelet  $\psi$ . In our study we use derivatives of the Gaussian function:  $\psi^{(n)} = d^n/dt^n e^{-(1/2)t^2}$ .

The wavelet transform is thus a cumulative measure of the variations in the heart rate signal over a region proportional to the wavelet scale, so study of the behavior of the wavelet values can reveal *intrinsic properties of the dynamics* masked by nonstationarity.

The second step of the cumulative variation magnitude analysis is to extract the instantaneous variation amplitudes of the wavelet-filtered signal by means of an analytic

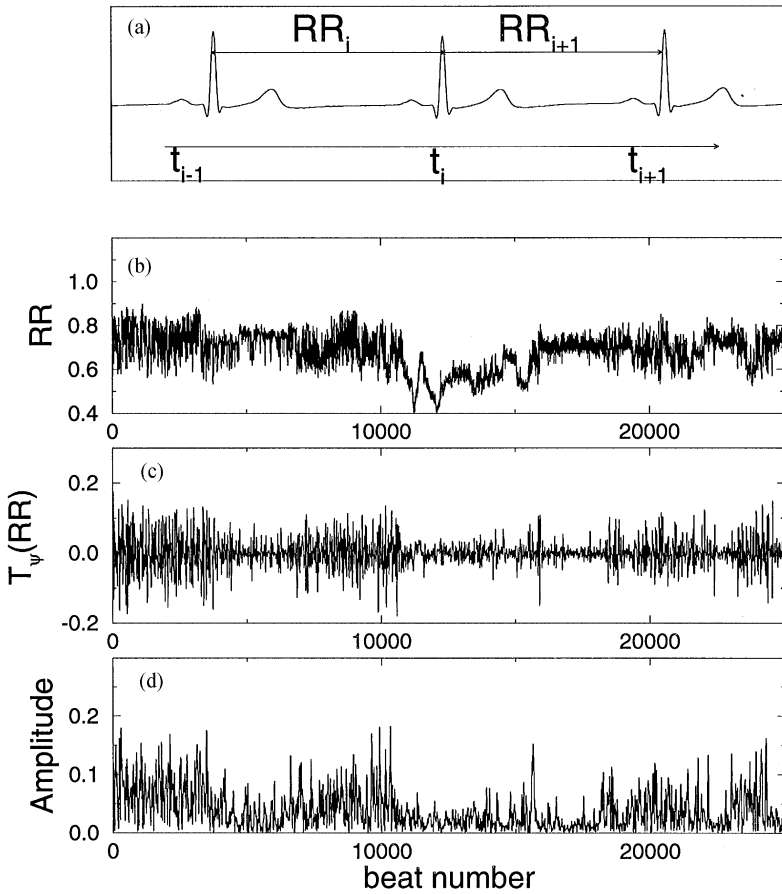


Fig. 4. (a) Segment of electrocardiogram showing beat-to-beat ( $RR_i$ ) intervals. (b) Plot of RR-time series vs. consecutive beat number for a period of 6 h ( $\approx 2.5 \times 10^4$  beats). Nonstationarity (patchiness) is evident over both long and short time scales. (c) Wavelet transform  $T_\psi(RR)$  of the RR-signal in (b) using the second derivative of the Gaussian function  $\psi^{(2)}$  as analyzing wavelet with scale  $a = 8$  beats. Non-stationarities related to constants and linear trends have been filtered out. (d) Instantaneous amplitudes  $A(t)$  of the wavelet-transform signal in (c);  $A(t)$ , which is calculated using the Hilbert transform, measures the cumulative variations in the interbeat intervals over an interval proportional to the wavelet scale  $a$ . Courtesy of P.Ch. Ivanov et al. [77].

signal approach [91,96] which also does not require stationarity. Let  $s(t)$  represent an arbitrary signal. The analytic signal, a complex function of time, is defined by  $S(t) = s(t) + i\tilde{s}(t) = A(t)e^{i\phi(t)}$ , where  $\tilde{s}(t)$  is the Hilbert transform [97] of  $s(t)$ . The instantaneous magnitude  $A(t)$  (Fig. 4d) and the instantaneous phase of the signal  $\phi(t)$  are defined as  $A(t) \equiv \sqrt{s^2(t) + \tilde{s}^2(t)}$  and  $\phi(t) \equiv \tan^{-1}(\tilde{s}(t)/s(t))$ .

We study the distribution of the amplitudes of the beat-to-beat variations (Fig. 5) for a group of healthy subjects ( $N = 18$ ; 5 male, 13 female; age: 20–50, mean - 34) and a group of subjects [98] with obstructive sleep apnea [99] ( $N = 16$  males;

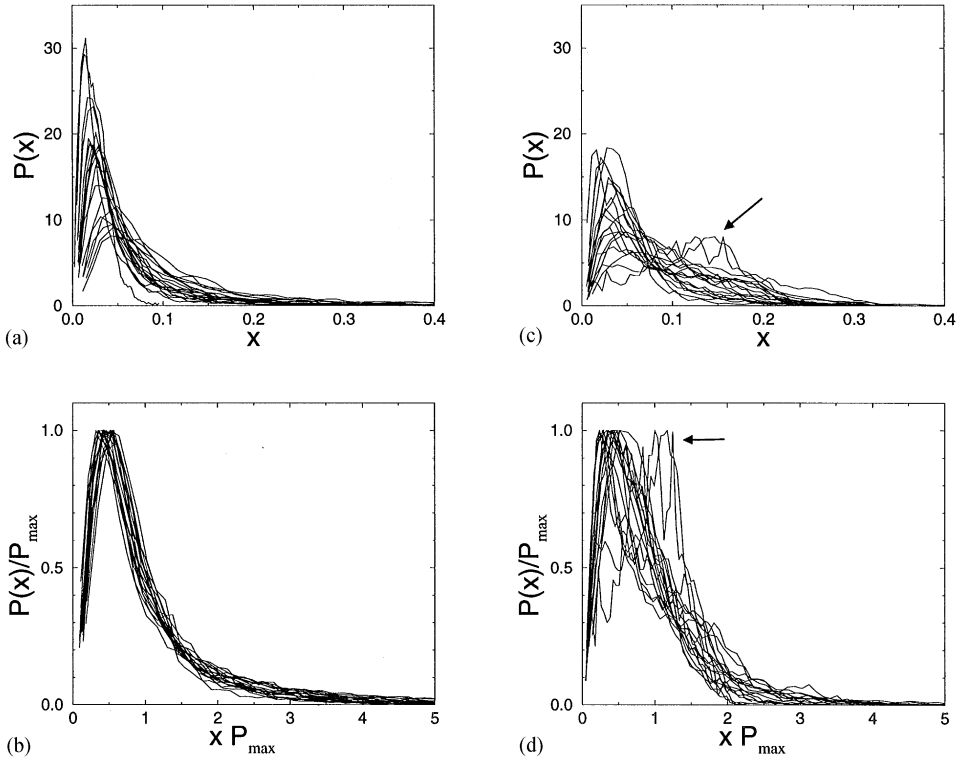


Fig. 5. (a) Probability distributions  $P(x)$  of the amplitudes of heart-rate variations  $x \equiv A(t)$  for a group of 18 healthy adults. Individual differences are reflected in the different average value and widths (standard deviations) of these distributions. All distributions are normalized to unit area. (b) Same probability distributions as in (a) after rescaling:  $P(x)$  by  $P_{\max}$ , and  $x$  by  $1/P_{\max}$  to preserve the normalization to unit area. The data points collapse onto a single curve. (c) Probability distributions for a group of 16 subjects with obstructive sleep apnea. We note that the second (rightward) peak in the distributions for the sleep apnea subjects corresponds to the transient emergence of characteristic pathologic oscillations in the heart rate associated with periodic breathing [99,105]. (d) Distributions for the apnea group after the same rescaling as in (b). These distributions *cannot* be well described by a single curve, indicating that the nonequilibrium dynamics are altered. Courtesy of P.Ch. Ivanov et al. [77].

age; 32 — 56, mean - 43). We begin by considering night phase (12 p.m. — 6 a.m.) records of interbeat intervals ( $\approx 10^4$  beats) for both groups to minimize nonstationarity due to changes in the level of activity. Inspection of the distribution functions of the amplitudes of the cumulative variations reveals marked differences between individuals (Fig. 5a). These discrepancies are not surprising given the underlying physiological differences among healthy subjects. To test the hypothesis that there is a hidden, possibly universal structure to these heterogeneous time series, we rescale the distributions and find for all healthy subjects that the data conform to a single scaled plot (“*data collapse*”) (Fig. 5b). We are able to describe the distributions using a single curve, indicating a robust, consistent scaling mechanism for the nonequilibrium dynamics. Such behavior is reminiscent of a wide class of well-studied physical systems with universal

scaling properties [100,4,14]. In contrast, the subjects with *sleep apnea* (Fig. 5c) show individual probability distributions which *fail* to collapse (Fig. 5d).

The absence of data collapse demonstrates deviation from the normal heart behavior. We note that direct analysis of interbeat interval histograms does *not* lead to data collapse or separation between the healthy and apnea group. Moreover, we find that the direct application of the Hilbert transform yielding the probability distribution of the instantaneous amplitudes of the original signal does *not* clearly distinguish healthy from abnormal cardiac dynamics. Hence, the crucial feature of the wavelet transform is that it extracts dynamical properties hidden in the cumulative variations. We observe for the healthy group good data collapse with *stable* scaling form for wavelet scales  $a = 2$  up to  $a = 32$  (Fig. 6c). However, for very small scales ( $a = 1, 2$ ) the average of the rescaled distributions of the apnea group is indistinguishable from the average of the rescaled distributions of the healthy group. Hence very high frequencies are equally present in the signals from both groups. Our analysis yields the most robust results when  $a$  is tuned to probe the collective properties of patterns with duration of  $\approx \frac{1}{2} - 1$  min in the time series ( $a = 8, 10$ ). The subtle difference between day and night phases is also best seen for this scale range.

We next analyze the distributions of the beat-to-beat variation amplitudes. For the healthy group, we find that these are well fit by the Gamma form:  $P(x) = (b^{v+1}/\Gamma(v+1))x^v e^{-bx}$ , where  $b = v/x_0$ ,  $\Gamma(v+1)$  is the Gamma function,  $x_0$  is the position of the peak  $P = P_{\max}$ , and  $v$  is the fitting parameter (Fig. 6a). Although individual distributions have different values of  $b$ , the homogeneous property of the functional form of  $P(x)$  leads to reduction of the independent variable  $x$  and parameter  $b$  to a single-scaled variable  $u \equiv bx$ . Instead of the data points falling on a family of curves, one for each value of  $b$ , we find the data points *collapse* onto a single curve given by the scaling function  $\tilde{P}(u) \equiv P(x)/b$ . Thus, it is sufficient to specify only one parameter  $b$  in order to characterize the heterogeneous heartbeat variations of each subject in this group.

We also analyzed heart-rate dynamics for the healthy subjects during day-time hours (noon – 6 p.m.). Our results indicate that the observed, apparently universal behavior holds not only for the night phase but for the day phase as well (Fig. 6b). Semilog plots of the averaged distributions show a systematic deviation from the exponential form (slower decay) in the tails of the night-phase distributions, whereas the day-phase distributions follow the exponential form over practically the entire range. Note that the tail of the observed distribution for the night phase indicates higher probability of larger variations in the healthy heart dynamics during sleep hours in comparison with the daytime dynamics [101].

It has been hypothesized [102] that even if the interbeat variations are different (e.g. smaller) during illness, the pattern of heart-rate variability might be otherwise very similar to that during health, so that the interbeat variations for normal and abnormal cardiac dynamics, once normalized, would have the same distribution. Our study clearly rejects this hypothesis, showing the presence of scaling in the distributions of the variation amplitudes for the healthy (Fig. 5b) and a breakdown of this scaling for abnormal dynamics (Fig. 5d). Moreover, the stability of this scaling form

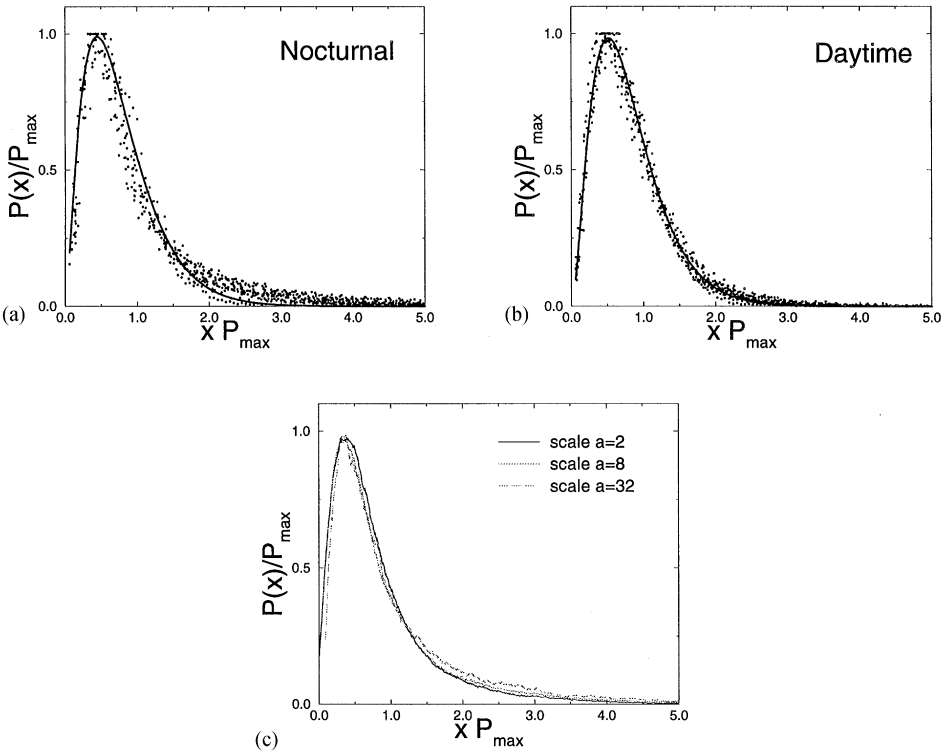


Fig. 6. (a) The solid line is an analytic fit of the rescaled distributions of the beat-to-beat variation amplitudes of the 18 healthy subjects during sleep hours to a stable Gamma distribution with  $\nu = 1.4 \pm 0.1$ . (b) Data for 6 h records of RR intervals for the day phase of the same control group of 18 healthy subjects demonstrate similar scaling behavior with a Gamma distribution and  $\nu = 1.8 \pm 0.1$ , thereby showing that the observed common structure for the healthy heart dynamics is not confined to the nocturnal phase. Semilog plots of the averaged distributions show a systematic deviation — crossover — in the tails of the night-phase distributions, whereas the day-phase distributions follow the exponential form over practically the entire range [101]. Note that the observed crossover for the night phase indicates higher probability of larger variations in the healthy heart dynamics during sleep hours in comparison with the daytime dynamics. (c) Group average of the rescaled distributions of the cumulative variation amplitudes for the healthy individuals during nocturnal hours. Note that the observed Gamma scaling is *stable* for a wide range of the wavelet transform scales  $a$ . Courtesy of P.Ch. Ivanov et al. [77].

(Fig. 6c) indicates that the underlying dynamical mechanisms regulating the healthy heart beat have similar statistical properties on different time scales. Such statistical self-similarity is an important characteristic of fractal objects. The wavelet decomposition of beat-to-beat heart-rate signals can be used to provide a visual representation of this fractal structure (Fig. 7). The wavelet transform, with its ability to remove local trends and to extract interbeat variations on different time scales, enables us to identify self-similar patterns (arches) in these variations even when the signals change as a result of background interference. Data from sick heart lack these patterns.

The study of Ivanov et al. [77] uncovers a previously unknown nonlinear feature of healthy heart-rate fluctuations. Prior reports of universal properties of the normal heart

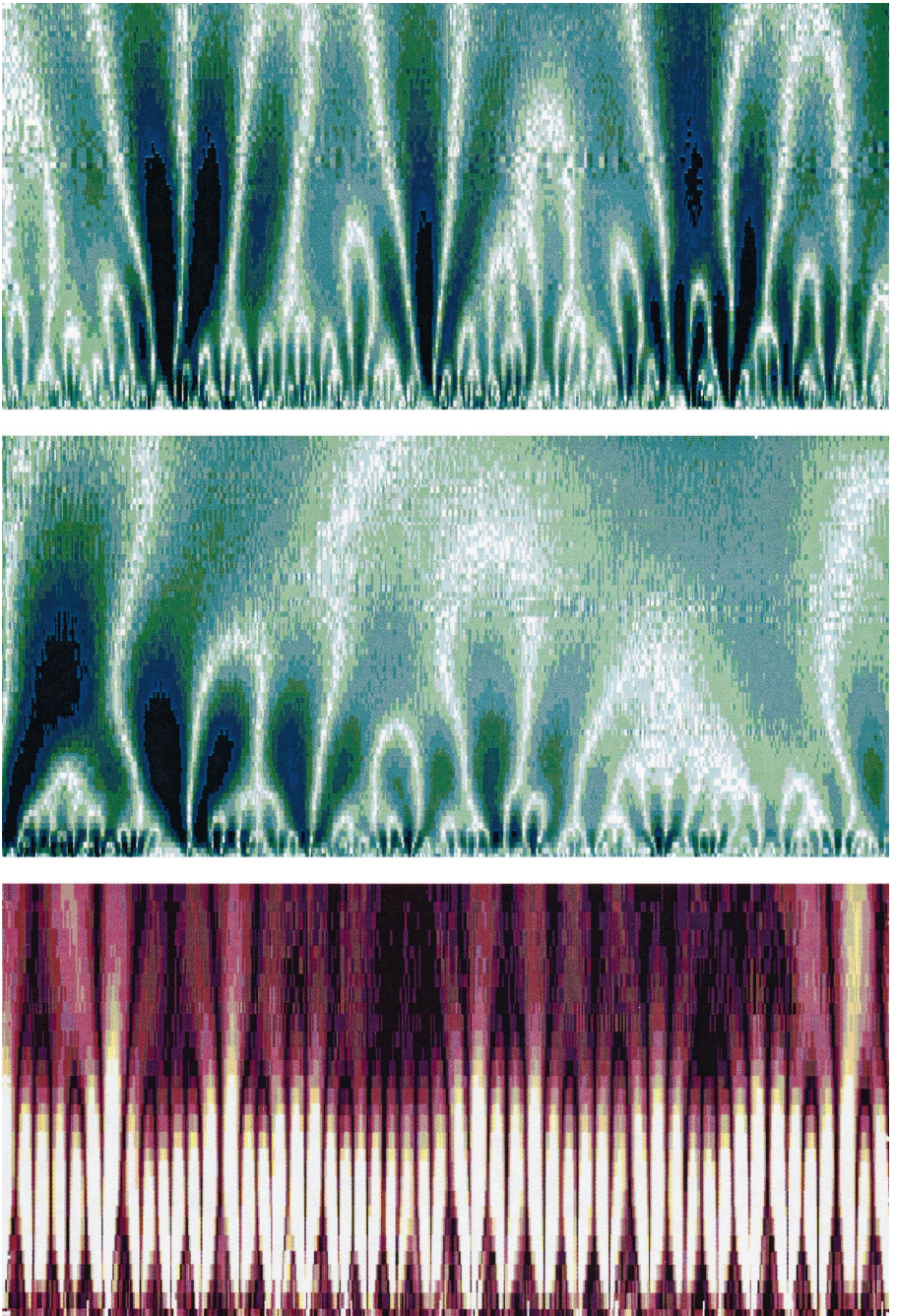


Fig. 7. Color-coded wavelet analysis of RR signals. The  $x$ -axis represents time ( $\approx 2000$  beats) and the  $y$ -axis indicates the scale of the wavelet used ( $a = 1, 2, \dots, 60$ ) with large scales at the top. The brighter colors indicate larger values of the wavelet amplitudes. The wavelet analysis performed with  $\psi^{(2)}$  (the Mexican hat) as an analyzing wavelet uncovers a hierarchical scale invariance (top panel) quantitatively expressed by the stability of the scaling form on Fig. 6(c). This wavelet decomposition reveals a self-similar fractal structure in the healthy cardiac dynamics — a magnification of the central portion of the top panel with 200 beats on the  $x$ -axis and wavelet scale  $a = 1, 2, \dots, 25$  on the  $y$ -axis shows identical branching patterns (middle panel). Loss of this fractal structure in cases with sleep apnea (lower panel). Courtesy of P.Ch. Ivanov et al. [103].

beat and other physiological signals relate to long-range correlations and power-law scaling. However, these properties, detected by Fourier and fluctuation analysis techniques, ignore information related to the phase interactions of component modes [103]. The nonlinear interaction of these modes accounts for the patchy, non-homogeneous appearance of the heartbeat time series and appears to be related to the recently reported multifractal properties of the heartbeat dynamics [104]. This finding suggests that for healthy individuals, there may be a common structure to this nonlinear phase interaction. The scaling property cannot be accounted for by activity, since we analyzed data from subjects during nocturnal hours. Moreover, it cannot be accounted for by sleep stage transitions, since we found a similar pattern during day-time hours. The basis of this robust temporal structure remains unknown and presents a new challenge to understanding nonlinear mechanisms of heartbeat control.

Additionally, we find that subjects with sleep apnea, a common and important instability of cardiopulmonary control, show a dramatic alteration in the scaling pattern – possibly related to pathologic mode locking associated with periodic breathing dynamics [105]. Thus, the dual use of wavelet and Hilbert transform techniques may be of practical diagnostic and prognostic value, and may also be applicable to a wide range of heterogeneous, “real world” physiological signals.

## 5. Scaling in weather fluctuations

It is well known in meteorology that the weather is persistent on short time scales. If one day is sunny and warm, there is a higher probability that the next day remains the same, and any “sophisticated” weather forecast must be better than the “trivial” one that predicts that the weather of tomorrow is the same as the weather of today [106,107].

To quantify the persistence, we have analyzed the records of the maximum daily temperatures  $T_i$  of the following 14 weather stations (the length of the records is written within the parentheses): Albany (90 y), Brookings (99 y), Huron (55 y), Luling (90 y), Melbourne (136 y), New York City (116 y), Pendleton (57 y), Prague (218 y), Sydney (117 y), Spokane (102 y), Tucson (97 y), Vancouver (93 y), Moscow (115 y), and St. Petersburg (111 y). The stations have been chosen randomly and represent the different climatological zones. We review the results from Koscielny et al. [25] and extend them using further complementary methods, such as Fast Fourier Transforms.

For each weather station, we consider the daily maximum temperature  $T_i$ . The total number  $N$  of days  $i$  available for a given weather station ranges typically from 20,000 days (Huron) to 80,000 days (Prague). For eliminating the periodic seasonal trends, we have considered the variations of  $T_i$ ,  $\Delta T_i = T_i - \bar{T}_i$ , from the mean maximum daily temperature  $\bar{T}_i$  for each calendary date  $i$ , say 1st of April, which has been obtained by averaging over all years in the temperature series. To analyze the  $\Delta T_i$  time series we have used several mathematical techniques: fluctuation analysis (FA), DFA, wavelets (WL1, WL2, WL3), and Fourier-analysis (for details see Ref. [25]). Our analysis

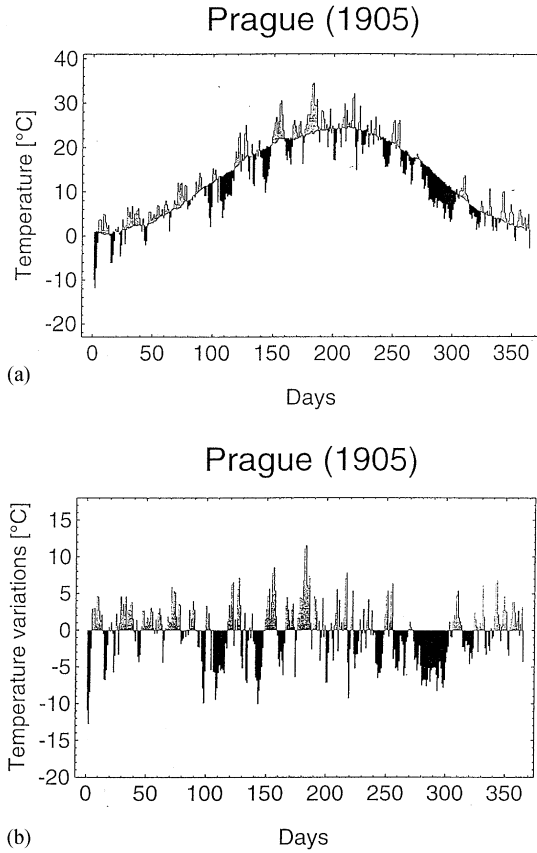


Fig. 8. (a) Maximum daily temperatures  $T_i$  for the year 1905 in the city of Prague. Values of  $T_i$  larger than the mean maximum temperature of the calendary date  $i$ ,  $\bar{T}_i$ , are indicated in light grey, and the values  $T_i < \bar{T}_i$  in black. Here  $\bar{T}_i$  has been obtained by averaging  $T_i$  over the period (1775–1992), consisting i.e. of 218 years. We have excluded the 29th February from the bissextile years. (b) Daily temperature variations  $\Delta T_i = T_i - \bar{T}_i$  for the same data shown in (a). Courtesy of E. Koscielny et al. [25].

suggests that the temperature fluctuations at days  $i$  and  $i + \ell$  are long-range power-law correlated, i.e., the correlation function behaves like

$$C(\ell) \equiv \langle \Delta T_i \Delta T_{i+\ell} \rangle \sim \ell^{-\gamma} \quad (4)$$

with an apparently universal exponent  $\gamma \cong 0.7$  for all weather stations considered. The brackets in Eq. (4) denote an average over all pairs of temperature data separated by  $\ell$  days,

$$\langle \Delta T_i \Delta T_{i+\ell} \rangle = \frac{1}{N - \ell} \sum_{i=1}^{N-\ell} \Delta T_i \Delta T_{i+\ell} \quad (5)$$

From our results we can conclude that, within the pertinent error bars, the power-law correlations set in after about one week (which is the typical time scale for a weather

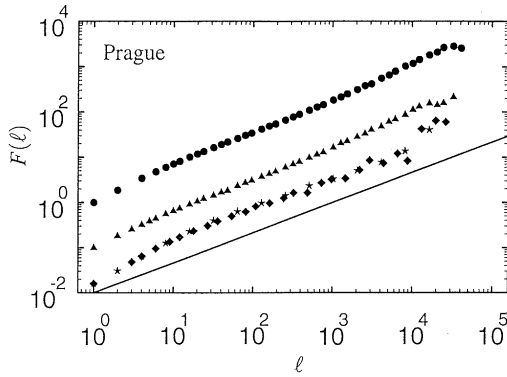


Fig. 9. Fluctuation analysis for the city of Prague. (a) FA (circles), (b) WL1 (triangles), WL2 (diamonds) and WL3 (stars). The straight lines have slopes  $\frac{2}{3}$  and are drawn as a guide to the eye. Courtesy of E. Koscielny et al. [25].

situation) and range at least over one decade of years. We did not find any evidence for a crossover to uncorrelated behavior at very large time scales, and cannot exclude the possibility that the range of the power-law correlations is larger than the range of the temperature series considered. In contrast to the universal behavior of the correlations, the distribution  $\mathcal{H}(\Delta T)$  of the temperature variations does not exhibit a universal form.

We show representative results for Prague (Fig. 8). We begin the analysis with the temperature series  $\{\Delta T_i\}$  for Prague which is the largest series (218 y) in this study.

Fig. 9 shows the fluctuation analysis for Prague obtained from the three methods. In the log–log plot, the DFA and wavelets curves are approximately straight lines for  $\ell > 10$  days, with a slope  $\alpha \cong 0.65$ . For  $\ell$  of the order of few days, the slope is a little larger. This result suggests, that there exists long-range persistence expressed by the power-law decay of the correlation function, with an exponent  $\gamma \cong 0.7$ . A closer look at these curves indicated that the effects of trends and correlations can be, to a certain extent, distinguished by the available methods. At about  $10^3$  days, the curves of FA and WL1 show a crossover towards a slightly larger exponent  $\alpha$ . This behavior can be interpreted as the effect of the warming of Prague due to urban development. In contrast, DFA, WL2, and WL3 yield approximate straight lines until about  $10^4$  days above which the data start to scatter. The systematic crossover at about  $10^3$  days does not occur here, since DFA, WL2, and WL3 eliminate the (roughly) linear trend of warming. For the Fourier-transform analysis, we obtain, in the double logarithmic representation, a straight line with the slope  $-(1 - \gamma) = 2\alpha - 1 = -0.3$ , consistent with the other methods. For  $f$  above  $f \cong 100$ , corresponding to  $\ell$  smaller than roughly 10 days, we see a crossover towards a larger exponent, in agreement with the previous analysis. Since the power spectrum analysis is limited to 2048 days, we cannot see the influence of trends involved in WL1. The direct evaluation of the autocorrelation function (Fig. 10) yields a consistent picture,  $C(\ell) \sim \ell^{-\gamma}$ . At very large time scales, scattering becomes dominant and hides the power-law behavior.

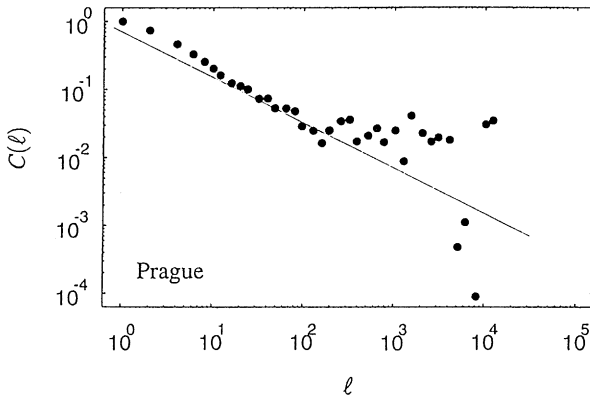


Fig. 10. The autocorrelation function  $C(\ell)$  for two days separated by  $\ell$  days, for the city of Prague. The straight line has slope  $\gamma = -\frac{2}{3}$  and is drawn as a guide to the eye. Courtesy of E. Koscielny et al. [25].

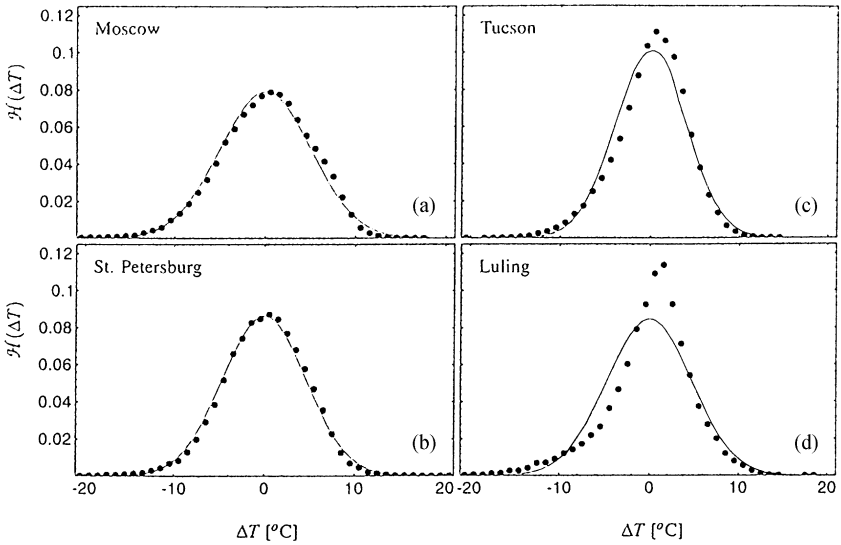


Fig. 11. The distribution of temperature variations  $\Delta T_i$  for: (a) Moscow (1880–1994, 115 years), (b) St. Petersburg (1884–1994, 111 years), (c) Tucson (Arizona) (1895–1991, 97 years) and (d) Luling (Texas) (1902–1991, 90 years). The lines are Gaussian fits with: (a)  $\sigma = 5.05^\circ\text{C}$ , (b)  $\sigma = 4.62^\circ\text{C}$ , (c)  $\sigma = 3.99^\circ\text{C}$  and (d)  $\sigma = 4.72^\circ\text{C}$ .

We obtain analogous results for the fluctuation functions for thirteen cities from all climate zones. The curves have the same features as the curves for Prague, and the exponents  $\alpha$  and  $\gamma$  seem to have almost the same values as for Prague. This may suggest the existence of a “global weather law”.

Finally, we have studied the normalized distribution function  $H(\Delta T)$  of the temperature variations  $\Delta T_i$  for the various meteorological stations. The distributions represent the number of day with  $\Delta T_i$  in the interval  $(\Delta T, \Delta T + \varepsilon)$  with  $\varepsilon = 1$  C divided by

the total number of days. Fig. 11 shows the result for four stations from two different climatological zones. Apparently, there is no universal behaviour for the distribution functions.

## Acknowledgements

We are grateful to many individuals, including R. Mantegna, F. Sciortino, M. Simons, M.G. Rosenblum, J. Fritsch-Yelle, R.M. Baevsky, L.A.N. Amaral, J. Mietus, E. Koscielny-Bunde, H.E. Roman, Y. Goldreich, H.J. Schellnhuber for major contributions to the results reviewed here which represent collaborative research efforts. We also wish to thank M. Azbel, C. Cantor, C. DeLisi, M. Frank-Kamenetskii, A.Yu. Grosberg, G. Huber, I. Labat, L. Liebovitch, G.S. Michaels, P. Munson, R. Nossal, R. Nussinov, R.D. Rosenberg, J.J. Schwartz, M. Schwartz, E.I. Shakhnovich, M.F. Shlesinger, N. Shworak, and E.N. Trifonov for valuable discussions. Partial support was provided by the National Science Foundation, National Institutes of Health (Human Genome Project), NIH/National Center for Research Resources (P41 RR13622), the G. Harold and Leila Y. Mathers Charitable Foundation, the National Heart, Lung and Blood Institute, the National Aeronautics and Space Administration (NASA), the Israel-USA Binational Science Foundation, and the Israel Academy of Sciences.

## References

- [1] B.B. Mandelbrot, *The Fractal Geometry of Nature*, W.H. Freeman, San Francisco, 1982.
- [2] A. Bunde, S. Havlin (Eds.), *Fractals and Disordered Systems*, Springer, Berlin, 1991.
- [3] A. Bunde, S. Havlin (Eds.), *Fractals in Science*, Springer, Berlin, 1994.
- [4] T. Vicsek, *Fractal Growth Phenomena*, 2nd Edition, World Scientific, Singapore, 1992.
- [5] T. Vicsek, M. Shlesinger, M. Matsushita (Eds.), *Fractals in Natural Sciences*, World Scientific, Singapore, 1994.
- [6] J. Feder, *Fractals*, Plenum, Press, New York, 1988.
- [7] D. Stauffer, H.E. Stanley, *From Newton to Mandelbrot: A Primer in Theoretical Physics*, Springer, Heidelberg, 1990.
- [8] E. Guyon, H.E. Stanley, *Les Formes Fractales*, (Palais de la Découverte, Paris, 1991) (English translation: *Fractal Forms*, Elsevier North-Holland, Amsterdam, 1991).
- [9] H.E. Stanley, N. Ostrowsky, (Eds.), *Random fluctuations and pattern growth: experiments and models*, Proceedings 1988 Cargèse NATO ASI, Kluwer Academic Publishers, Dordrecht, 1988.
- [10] H.E. Stanley, N. Ostrowsky, (Eds.), *Correlations and connectivity: geometric aspects of physics, chemistry and biology*, Proceedings 1990 Cargèse Nato ASI, Series E: Applied Sciences, Kluwer, Dordrecht, 1990.
- [11] J.M. Garcia-Ruiz, E. Louis, P. Meakin, L. Sander (Eds.), *Growth patterns in physical sciences and biology*, Proceedings of the 1991 NATO Advanced Research Workshop, Granada, Spain, October 1991, Plenum, New York, 1993).
- [12] B.J. West, *Fractal Physiology and Chaos in Medicine*, World Scientific, Singapore, 1990.
- [13] A. Yu. Grosberg, A.R. Khokhlov, *Statistical Physics of Macromolecules*, (translated by Y.A. Atanov) AIP Press, New York, 1994.
- [14] J.B. Bassingthwaighte, L.S. Liebovitch, B.J. West, *Fractal Physiology*, Oxford University Press, New York, 1994.
- [15] A.-L. Barabási, H.E. Stanley, *Fractal Concepts in Surface Growth*, Cambridge University Press, Cambridge, 1995.

- [16] C.-K. Peng, S.V. Buldyrev, A.L. Goldberger, S. Havlin, F. Sciortino, M. Simons, H.E. Stanley, *Nature* 356 (1992) 168.
- [17] B. Suki, A.-L. Barabasi, Z. Hantos, F. Petak, H.E. Stanley, *Nature* 368 (1994) 615.
- [18] A.-L. Barabasi, S.V. Buldyrev, H.E. Stanley, B. Suki, *Phys. Rev. Lett.* 76 (1996) 2192.
- [19] M. Kobayashi, T. Musha, *IEEE Trans. Biomed. Eng.* 29 (1982) 456.
- [20] B.J. West, A.L. Goldberger, *J. Appl. Physiol.* 60 (1986) 189.
- [21] B.J. West, A.L. Goldberger, *Am. Sci.* 75 (1987) 354.
- [22] C.-K. Peng, J. Mietus, J.M. Hausdorff, S. Havlin, H.E. Stanley, A.L. Goldberger, *Phys. Rev. Lett.* 70 (1993) 1343.
- [23] C.-K. Peng, S. Havlin, H.E. Stanley, A.L. Goldberger, *Chaos* 5 (1995) 82.
- [24] H.A. Makse, S. Havlin, H.E. Stanley, *Nature* 377 (1995) 608.
- [25] E. Koscielny-Bunde, A. Bunde, S. Havlin, H.E. Roman, Y. Goldreich, H.-J. Schellnhuber, Indication of a universal persistence law governing atmospheric variability, *Phys. Rev. Lett.* 81 (1998) 729.
- [26] R.N. Mantegna, H.E. Stanley, *Phys. Rev. Lett.* 73 (1994) 2946.
- [27] R.N. Mantegna, H.E. Stanley, *Nature* 376 (1995) 46.
- [28] M.H.R. Stanley, L.A. Amaral, S.V. Buldyrev, S. Havlin, H. Leschhorn, P. Maass, M.A. Salinger, H.E. Stanley, *Nature* 379 (1996) 804.
- [29] S. Tavaré, B.W. Giddings, in: M.S. Waterman (Ed.), *Mathematical Methods for DNA Sequences*, CRC Press, Boca Raton, 1989, pp. 117–132.
- [30] J.D. Watson, M. Gilman, J. Witkowski, M. Zoller, *Recombinant DNA*, Scientific American Books, New York, 1992.
- [31] E.W. Montroll, M.F. Shlesinger, The wonderful world of random walks, in: J.L. Lebowitz, E.W. Montroll (Eds.), *Nonequilibrium Phenomena II. From Stochastics to Hydrodynamics*, North-Holland, Amsterdam, 1984, pp. 1–121.
- [32] G.H. Weiss, *Random Walks*, North-Holland, Amsterdam, 1994.
- [33] S. Havlin, R. Selinger, M. Schwartz, H.E. Stanley, A. Bunde, *Phys. Rev. Lett.* 61 (1988) 1438.
- [34] C.-K. Peng, S. Havlin, M. Schwartz, H.E. Stanley, *Phys. Rev. A* 44 (1991) 2239.
- [35] M. Araujo, S. Havlin, G.H. Weiss, H.E. Stanley, *Phys. Rev. A* 43 (1991) 5207.
- [36] S. Prakash, S. Havlin, M. Schwartz, H.E. Stanley, *Phys. Rev. A* 46 (1992) R1724.
- [37] M.Y. Azbel, *Phys. Rev. Lett.* 31 (1973) 589.
- [38] W. Li, K. Kaneko, *Europhys. Lett.* 17 (1992) 655.
- [39] C.L. Berthelsen, J.A. Glazier, M.H. Skolnick, *Phys. Rev. A* 45 (1992) 8902.
- [40] S.M. Ossadnik, S.V. Buldyrev, A.L. Goldberger, S. Havlin, R.N. Mantegna, C.-K. Peng, M. Simons, H.E. Stanley, *Biophys. J.* 67 (1994) 64.
- [41] H.E. Stanley, S.V. Buldyrev, A.L. Goldberger, S. Havlin, S.M. Ossadnik, C.-K. Peng, M. Simons, *Fractals* 1 (1993) 283–301.
- [42] M.Y. Azbel, *Biopolymers* 21 (1982) 1687.
- [43] P.J. Munson, R.C. Taylor, G.S. Michaels, *Nature* 360 (1992) 636.
- [44] I. Amato, *Science* 257 (1992) 747.
- [45] A. Yu. Grosberg, Y. Rabin, S. Havlin, A. Neer, *Europhys. Lett.* 23 (1993) 373.
- [46] S. Nee, *Nature* 357 (1992) 450.
- [47] R. Voss, *Phys. Rev. Lett.* 68 (1992) 3805.
- [48] R. Voss, *Fractals* 2 (1994) 1.
- [49] V.V. Prabhu, J.-M. Claverie, *Nature* 357 (1992) 782.
- [50] C.A. Chatzidimitriou-Dreismann, D. Larhammar, *Nature* 361 (1993) 212.
- [51] D. Larhammar, C.A. Chatzidimitriou-Dreismann, *Nucleic Acids Res.* 21 (1993) 5167.
- [52] C.A. Chatzidimitriou-Dreismann, R.M.F. Streffer, D. Larhammar, *Biochim. Biophys. Acta* 1217 (1994) 181.
- [53] C.A. Chatzidimitriou-Dreismann, R.M.F. Streffer, D. Larhammar, *Eur. J. Biochem.* 224 (1994) 365.
- [54] S. Karlin, V. Brendel, *Science* 259 (1993) 677.
- [55] C.-K. Peng et al., *Phys. Rev. E* 49 (1994) 1685.
- [56] S.V. Buldyrev, A.L. Goldberger, S. Havlin, R.N. Mantegna, M.E. Matsu, C.-K. Peng, M. Simon, H.E. Stanley, *Phys. Rev. E* 51 (1995) 5084.
- [57] A. Arneodo, E. Bacry, P.V. Graves, J.F. Muzy, *Phys. Rev. Lett.* 74 (1995) 3293–3296.
- [58] A. Arneodo, Y. d'Aubenton-Carafa, C. Thermes, *Physica D* 96 (1996) 291.

- [59] C. Thermes, Y. d'Aubenton-Carafa, B. Audit, C. Vaillant, J.F. Muzy, A. Arneodo, Universal multi-scale structural properties of genomic DNA revealed by wavelet analysis, pre-print, 1999.
- [60] W.B. Cannon, *Physiol. Rev.* 9 (1929) 399.
- [61] C. Bernard, *Les Phénomènes de la Vie*, Paris, 1878.
- [62] B. Van der Pol, J. van der Mark, *Philos. Mag.* 6 (1928) 763.
- [63] W.B. Cannon, *Physiol. Rev.* 9 (1929) 399.
- [64] R.M. Berne, M.N. Levy, *Cardiovascular Physiology*, 6th Edition, C.V. Mosby, St. Louis, 1996.
- [65] M. Malik, A.J. Camm, (Eds.) *Heart Rate Variability*, Futura, Armonk NY, 1995.
- [66] G.E.P. Box, G.M. Jenkins, G.C. Reinsel, *Time Series Analysis: Forecasting and Control*, Prentice-Hall, Englewood Cliffs, NJ, 1994.
- [67] M.F. Shlesinger, *Ann. NY Acad. Sci.* 504 (1987) 214.
- [68] L.S. Liebovitch, *Biophys. J.* 55 (1989) 373.
- [69] M. Mackey, L. Glass, *Science* 197 (1977) 287.
- [70] M.M. Wolf et al., *Med. J. Aust.* 2, (1978) 52.
- [71] R.I. Kitney et al., *Automedica* 4 (1982) 141.
- [72] L. Glass, P. Hunter, A. McCulloch (Eds), *Theory of Heart*, Springer, New York, 1991.
- [73] J. Kurths et al., *Chaos* 5 (1995) 88–94.
- [74] G. Sugihara et al., *Proc. Natl. Acad. Sci. USA* 93 (1996) 2608–2613.
- [75] R.I. Kitney, O. Rompelman, *The Study of Heart-Rate Variability*, Oxford Univ. Press, London, 1980.
- [76] J.P. Saul et al., P. Albrecht, D. Berger, R.J. Cohen, *Computers in Cardiology*, IEEE Computer Society Press, Washington DC, 1987, p. 419.
- [77] P.Ch. Ivanov, M.G. Rosenblum, C.-K. Peng, J. Mietus, S. Havlin, H.E. Stanley, A.L. Goldberger, *Nature* 383 (1996) 323.
- [78] L.A. Lipsitz et al., *Circulation* 81 (1990) 1803.
- [79] D.T. Kaplan et al., *Biophys. J.* 59 (1991) 945.
- [80] N. Iyengar et al., *Am. J. Physiol.* 271 (1996) R1078.
- [81] M.F. Shlesinger, B.J. West, *Random Fluctuations and Pattern Growth: Experiments and Models*, Kluwer Academic Publishers, Boston, 1988.
- [82] H. Moelgaard et al., *Am. J. Cardiol.* 68 (1991) 777.
- [83] P.Ch. Ivanov et al., Sleep-wake differences in scaling behavior of the human heartbeat: analysis of terrestrial and long-term space flight data, *Europhys. Lett.*, in press.
- [84] A.L. Goldberger et al., *Am. Heart J.* 128 (1994) 202.
- [85] R.W. Peters et al., *J. Am. Coll. Cardiol.* 23 (1994) 283.
- [86] S. Behrens et al., *Am. J. Cardiol.* 80 (1997) 45.
- [87] P.Ch. Ivanov, L.A.N. Amaral, A.L. Goldberger, H.E. Stanley, *Europhys. Lett.* 43 (1998) 363.
- [88] R.I. Kitney, D. Linkens, A.C. Selman, A.H. McDonald, *Automedica* 4 (1982) 141.
- [89] A.L. Goldberger, D.R. Rigney, J. Mietus, E.M. Antman, S. Greenwald, *Experientia* 44 (1988) 983.
- [90] A.L. Goldberger, *Lancet* 347 (1996) 1312.
- [91] D. Panter, *Modulation, Noise and Spectral Analysis*, McGraw-Hill, New York, 1965.
- [92] S. Akselrod, D. Gordan, F.A. Ubel, D.C. Shannon, A.C. Barger, R.J. Cohen, *Science* 213 (1981) 220–222.
- [93] A. Grossmann, J. Morlet, *Mathematics and Physics, Lectures on Recent Results*, World Scientific, Singapore, 1985.
- [94] I. Daubechies, *Commun. Pure Appl. Math.* 41 (1988) 909–996.
- [95] J.F. Muzy, E. Bacry, A. Arneodo, *Int. J. Bifurc. Chaos* 4 (1994) 245.
- [96] L.A. Vainshtein, D.E. Vakman, *Separation of Frequencies in the Theory of Oscillations and Waves*, Nauka, Moscow, 1983.
- [97] D. Gabor, *J. Inst. Electr. Eng.* 93 (1946) 429–457.
- [98] MIT-BIH Polysomnographic Database CD-ROM, 2nd Edition, MIT-BIH Database Distribution, Cambridge, 1992.
- [99] C. Guilleminault, S. Connolly, R. Winkle, K. Melvin, A. Tilkian, *Lancet* 1 (1984) 126–131.
- [100] H.E. Stanley, *Introduction to Phase Transitions and Critical Phenomena*, Oxford University Press, London, 1971.
- [101] P.Ch. Ivanov, M.G. Rosenblum, C.-K. Peng, J. Mietus, S. Havlin, H.E. Stanley, A.L. Goldberger, *Scaling and universality in heart rate variability distributions*, *Physica A [Proc. Bar-Ilan Conf.]* 249 (1998) 587.
- [102] A.A. Aghili et al., *phys. Rev. Lett.* 74 (1995) 1254.

- [103] P.Ch. Ivanov et al, in: J.C. van den Berg (Ed.), *Wavelets in Physics*, Cambridge University Press, Cambridge, 1998.
- [104] P.Ch. Ivanov, L.A.N. Amaral, A.L. Goldberger, S. Havlin, M.G. Rosenblum, Z. Struzik, H.E. Stanley, *Nature* 399 (1999) 461.
- [105] L.A. Lipsitz et al., *Br. Heart J.* 74 (1995) 340–396.
- [106] O.M. Essenwagner, *General Climatology. Elements of statistical analysis*, Vol. 1B, in: H.E. Landsberg (Ed.), *Word Survey of Climatology*, Elsevier, Amsterdam, 1986.
- [107] S.B. Newman, *Weather Forecasting* 6 (1991) 111.
- [108] S.V. Buldyrev, A.L. Goldberger, S. Havlin, C.-K. Peng, M. Simons, H.E. Stanley, *Phys. Rev. E* 47 (1993) 4514.